Development 136, 3549-3556 (2009) doi:10.1242/dev.037747

Self-renewing epiblast stem cells exhibit continual delineation of germ cells with epigenetic reprogramming in vitro

Katsuhiko Hayashi and M. Azim Surani*

Pluripotent epiblast stem cells (EpiSCs) derived from postimplantation embryos exhibit properties that are characteristically different when compared with pluripotent embryonic stem cells (ESCs) derived from mouse blastocysts. However, EpiSCs are relatively less well characterised compared with ESCs. In particular, the relationship between EpiSCs and primordial germ cells (PGCs) is unknown, and is worthy of investigation because PGCs originate from postimplantation epiblast cells in vivo. We show that EpiSCs have an infinite capacity for generating PGCs, under conditions that sustain their pluripotency and self-renewal. These PGCs generated in vitro show appropriate transcriptional and epigenetic reprogramming events and are able to develop further into late germ cells. Notably, the PGCs can, in turn, be induced to undergo dedifferentiation into pluripotent embryonic germ cells (EGCs), which resemble ESCs and not the EpiSC from which they are derived. Our observations demonstrate intrinsic reprogramming during specification of PGCs that results in the erasure of epigenetic memory of EpiSCs following reactivation of the X-chromosome, DNA demethylation and re-expression of key pluripotency genes. This study provides novel insights into the nature and properties of EpiSCs, and introduces an in vitro model system that will be useful for investigations on PGC specification and on mechanisms regulating epigenetic reprogramming in germ cells.

KEY WORDS: Primordial germ cells, Pluripotency, EpiSC, Blimp1 (Prdm1), Stella

INTRODUCTION

The pluripotent state is first established in the inner cell mass (ICM) of blastocysts that develops from the totipotent zygote (Niwa, 2007; Surani et al., 2007). During subsequent postimplantation development, the epiblast cells originating from the ICM commence differentiation into diverse somatic cells, but these cells also give rise to primordial germ cells (PGCs). Furthermore, it is possible to generate pluripotent stem cells in vitro under appropriate culture conditions from the ICM, the postimplantation epiblast and PGCs; these are embryonic stem cells (ESCs), epiblast stem cells (EpiSCs) and embryonic germ cells (EGCs), respectively (Brons et al., 2007; Evans and Kaufman, 1981; Matsui et al., 1992; Resnick et al., 1992; Tesar et al., 2007). Although all these pluripotent stem cells share some common properties, such as expression of key pluripotent-associated genes including *Oct4*, *Nanog* and *Sox2*, EpiSCs in particular differ significantly from ESCs and EGCs in their epigenetic state and gene transcription profile (Brons et al., 2007; Guo et al., 2009; Hayashi et al., 2008; Tesar et al., 2007).

Notably, EpiSCs inherit many properties from epiblast cells, including an inactive X chromosome (in female lines) and higher expression levels of genes such as *Fgf5*, *Lefty1* and *Cer1*, as well as the repression or lower expression of some pluripotency genes. By contrast, the epigenetic state and gene expression profile of EGCs is strikingly similar to that of ESCs because the specification of PGCs involves epigenetic reprogramming that results in the erasure of the epigenetic memory of epiblast cells (Hayashi and Surani, 2009). This includes reactivation of the inactive X chromosome (Chuva de Sousa Lopes et al., 2008; de Napoles et al., 2007; Sugimoto and Abe, 2007), repression of the somatic programme, re-expression of many pluripotency-specific genes, and chromatin modifications and DNA demethylation (Ancelin et al., 2006; Hajkova et al., 2008; Ohinata et al., 2005; Seki et al., 2005; Seki et al., 2007). The changes that occur during the dedifferentiation of PGCs to EGCs convert unipotent germ cells to pluripotent stem cells, and follow from the downregulation of Blimp1 and the translocation of Prmt5 from the nucleus to the cytoplasm (Durcova-Hills et al., 2008). Thus, while PGCs represent a unipotent lineage, their epigenetic state is closer to that of the ICM of blastocysts, which explains why EGCs are like ESCs and unlike EpiSCs.

Investigations on many aspects of the underlying mechanism of epigenetic reprogramming during PGC specification would be facilitated by an in vitro system, especially if it is possible to generate large numbers of PGCs. In this respect, EpiSCs are of particular interest, as they are derived from epiblast cells from which PGCs originate in vivo. Here, we analysed EpiSCs carrying Blimp1-GFP or Stella-GFP reporters; Blimp1 (also known as Prdm1) is the key determinant of PGCs in mice, and the earliest known marker of PGC precursors (Ohinata et al., 2005). Stella (Dppa3 – Mouse Genome Informatics) is detected in Blimp1-positive cells at the end of the PGC specification process (Hayashi et al., 2007; Kurimoto et al., 2008; Ohinata et al., 2005). Our analyses revealed that it is possible to generate PGC precursors and fully specified germ cells from EpiSCs, which occurs following appropriate epigenetic reprogramming events and changes in the gene expression profile. Importantly, we found continuous delineation of PGCs from EpiSCs under conditions that retain their capacity for self-renewal and pluripotent state. Thus, EpiSCs are a potential source for a large number of PGCs, and they provide an important in vitro system for studies on the germ cell lineage.

MATERIALS AND METHODS

Embryo collection and cell culture

Epiblast tissue was collected on embryonic day (E) 6.5 embryos from 129SvEv females crossed with *Blimp1-Gfp*-BAC or *Stella-Gfp*-BAC transgenic males (Ohinata et al., 2005; Payer et al., 2006). EpiSCs were

Wellcome Trust Cancer Research UK Gurdon Institute, The Henry Wellcome Building for Cancer and Developmental Biology, University of Cambridge, Tennis Court Road, Cambridge CB2 1QN, UK.

*Author for correspondence (a.surani@gurdon.cam.ac.uk)

Accepted 1 September 2009

derived from the epiblast as described previously with slight modification (Brons et al., 2007). Briefly, E6.5 epiblasts were stripped from the visceral endoderm (VE), and cultured in chemically defined medium (Brons et al., 2007) on mouse embryonic fibroblasts (MEFs). After several passages, the culture medium was replaced with N2B27 medium supplemented with 20% KSR, 2 ng/ml recombinant human activin A (Peprotech) and 12 ng/ml bFGF (Invitrogen).

Immunofluorescence and FACS analysis

For FACS analysis, single cell suspensions of EpiSCs were analysed and sorted by FACSort with CELLQUEST software (BD Bioscience) and FACSAria (BD Bioscience). For SSEA1 staining, single cells were incubated with PE-conjugated anti-SSEA1 antibody (R&D Systems), according to the manufacturer's instructions. For intracytoplasmic staining, EpiSCs were fixed with 4% paraformaldehyde, permeabilised with 0.1% Triton X-100, and stained with mouse anti-Oct4 mAb (BD Bioscience) followed by Alexa 568-conjugated goat anti-mouse IgG (Invitrogen). To intensify the signal, these samples were stained again with Alexa568-conjugated donkey anti-goat IgG (Invitrogen). For immunofluorescence analysis, cells were fixed with 4% paraformaldehyde, washed with PBS and then stained with appropriate primary antibodies: rabbit polyclonal anti-Stella antibody, which was raised against a synthetic peptide; rat anti-GFP monoclonal antibody (mAb; Nacalai tesque); mouse anti-Oct4 mAb (BD Bioscience); rabbit anti-Mvh polyclonal antibody (Abcam) and rabbit anti-Sycp3 polyclonal antibody (kindly provided from Dr Chuma, Kyoto University, Japan). Secondary antibodies conjugated with Alexa488, Alexa568 or Alexa647 were used to detect the binding of the primary antibodies to specific cells. DAPI (4,6′-diamidino-2-phenylindole) was used for staining nuclei. The stained cells were analysed by a BioRad (Hercules, CA, USA) Radiance 2000 confocal microscope.

PGC induction and EG cell derivation

To promote differentiation of EpiSCs, BMP4 (R&D Systems) was added to the culture medium at 500 ng/ml. The cells were washed after 24 hours and cultured with Noggin (R&D Systems) at 250 ng/ml and chordin (R&D Systems) at 1.25 μg/ml. All culture media was supplemented with activin A and bFGF. Cells were analysed at 48 hours after the addition of BMP4. EGC derivation from Stella$^+$ EpiSCs was performed as described previously, with slight modifications (Durcova-Hills and Surani, 2008). Briefly, FACS-sorted Stella$^+$ EpiSCs (sorted at a rate of 3000 cells/well) were cultured on mitotically inactive Sl^4-m220 in DMEM supplemented with 15% FCS, nonessential amino acids, 2 mM L-glutamine, penicillin/streptomycin, 1 mM sodium pyruvate, 50 μM 2-mercaptoethanol, 1000 U/ml LIF (Chemicon International) and 25 ng/ml bFGF. After 5-6 days of culture, the resulting EGC-like colonies were dissociated by trypsin treatment and spread on MEF. After derivation, EGCs were cultured on MEFs in the medium without bFGF.

Co-culture of PGCs with gonadal cells

For the culture of in vitro-derived PGCs with gonadal cells, female gonads were collected from E12.5 embryos. A small number of the collected gonads were cut into small pieces and put on transwell inserts (Falcon) in DMEM supplemented with 20% fetal calf serum (FCS), 2 mM L-glutamine, and penicillin/streptomycin. In addition, 10-12 gonads were dissociated by treatment with trypsin and mixed with the FACS-sorted 3000 Stella-GFP$^+$ PGCs. After centrifugation, the cell suspension was transferred into a small drop of medium on a petri dish. The cells were brought together to the centre of the dish by gently rocking the culture dish for 1 minute by hand. The 'centralised' aggregate of cells was aspirated with a minimum volume of medium using a glass pipette, and transferred through the gaps present between the small pieces of gonads on the transwell inserts. The culture medium was subsequently changed every day.

RT-PCR analysis

For quantitative PCR (Q-PCR) analysis, cDNA was synthesised from total RNA using Superscript II and oligo d(T) primers. Single-cell cDNA preparation was performed as described previously (Kurimoto et al., 2007). cDNA was used for Q-PCR reactions using Sybr Green master mix (Qiagen) and specific primers. Primer sequences used in this study are shown in Table S1 in the supplementary material.

RESULTS AND DISCUSSION

We first derived three separate EpiSC lines carrying the Blimp1-BAC-GFP reporter (henceforth called Blimp1-EpiSC) (Ohinata et al., 2005), as this gene is the key determinant and the earliest marker of PGC precursors. Blimp1-EpiSC lines were similar to non-transgenic EpiSCs, and showed the capacity for extensive self-renewal while retaining expression of the pluripotent genes for at least 60 passages (data not shown). We first detected Blimp1-GFP expression at the start of the derivation process in almost all epiblast cells after 2 days of culture, but this expression became gradually downregulated (data not shown). However, even after the completion of the derivation process, we detected Blimp1-GFP expression in a significant proportion (10 to 50%) of the self-renewing Blimp1-EpiSCs (Fig. 1A); some of these GFP-positive cells were also Oct4 positive (Fig. 1B). We observed Blimp1-GFP expressing cells in all the established Blimp1-EpiSC lines. However, the proportion of Blimp1-GFP$^+$ cells was variable, which was partly due to their spontaneous differentiation, as the frequency of the Blimp1-GFP$^+$ cells was proportional to the morphological state of the colonies, which apparently increased whenever we observed morphologically differentiated colonies (see below). Notably, quantitative PCR (Q-PCR) analysis of FACS-sorted Blimp1-GFP$^+$ cells revealed the expression of key markers of early PGCs, including *Nanos3*, *Prdm14* and *Dnd1* (Fig. 1C). Furthermore, we observed repression of *Hoxa1* in the Blimp1-GFP$^+$ cells, which is also one of the key features of PGC specification in vivo (Saitou et al., 2002). More significantly, we also detected transcripts of *Stella* (also known as *Dppa3*), which is a definitive marker of PGCs, exclusively in the Blimp1-GFP$^+$ cells (Saitou et al., 2002; Sato et al., 2002) (Fig. 1C). These observations suggest that, amongst the Blimp1-GFP$^+$ cells, we were detecting early PGCs originating from the EpiSCs in culture.

Additional analysis of the Blimp1-GFP$^+$ cells, however, revealed expression of *Gata4* and *Gata6* (Fig. 1C), which are markers of the visceral endoderm (VE) at early postimplantation stage. This is perhaps not surprising as Blimp1-GFP expression is also detected in the VE of E6.25 embryos (Ohinata et al., 2005). This suggests that the Blimp1-GFP$^+$ cells we observed in vitro are composed of at least the PGC precursors and VE cells that are generated spontaneously in EpiSC culture. We could use Oct4 and/or SSEA1 expression as additional markers to distinguish between PGC precursors and VE, as PGC precursors would express these markers, whereas the VE would instead be expected to show expression of Gata4/Gata6. Indeed, immunostaining and single cell Q-PCR revealed mutually exclusive expression of Oct4 and Gata4/Gata6 in the Blimp1-GFP$^+$ cells (see Fig. S1 in the supplementary material). In additional immunostaining studies, we also found that the SSEA1$^+$/Blimp1-GFP$^+$ cells were positive for the PGC markers, and lacked expression of *Gata4/Gata6* (see Fig. S2 in the supplementary material). FACS analysis revealed that between 6 and 10% of the cells in Blimp1-EpiSC cultures were Oct4$^+$/Blimp1-GFP$^+$ putative PGC precursors (Fig. S1 in the supplementary material). Thus, a combination of Blimp1-GFP with either Oct4 or SSEA1 can be used as markers to detect and isolate PGC precursors. Notably, these germ cell precursors are yet to undergo the full process of specification before being irreversibly committed as founder PGCs. The final commitment to PGC fate is evident by the expression of *Stella*, a PGC-specific marker.

To follow the final events associated with the establishment of germ cells from PGC precursors originating from EpiSCs, we used *Stella* as a reporter by generating four EpiSC lines from Stella-BAC-GFP reporter mice (Stella-EpiSCs) (Payer et al.,

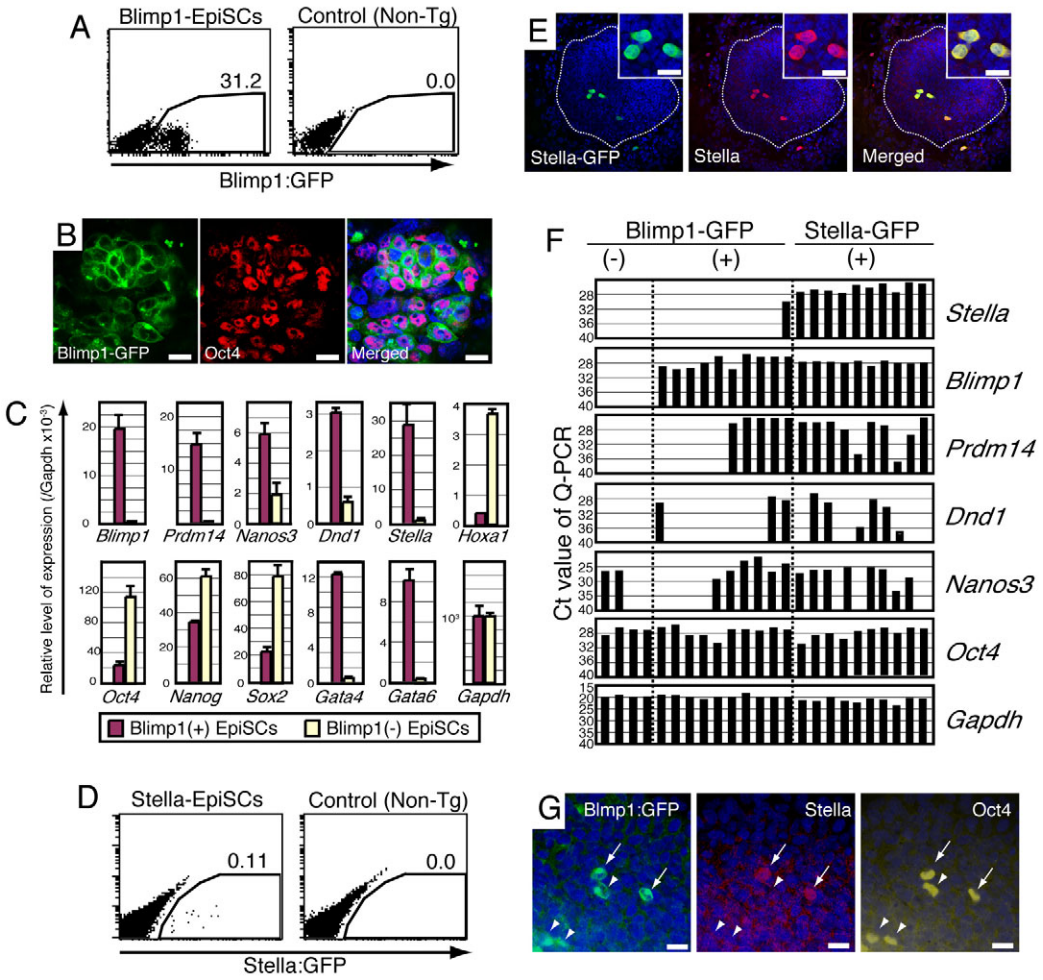

Fig. 1. Detection of PGCs in EpiSC cultures. (**A**) FACS analysis of Blimp1-EpiSCs and detection of Blimp1-GFP$^+$ cells (%) in a dot plot, compared with a non-transgenic control. (**B**) Co-expression of Blimp1-GFP and Oct4 in Blimp1-EpiSCs detected by immunofluorescence analysis using antibodies as indicated, and DAPI for nuclei (blue). (**C**) Q-PCR analysis of early PGC markers and pluripotent genes in FACS-sorted Blimp1-GFP$^+$ and Blimp1-GFP$^-$ populations from Blimp1-EpiSCs. Relative levels of gene expression were obtained with reference to *Gapdh* expression. (**D**) FACS analysis of Stella-GFP$^+$ cells (%) in a dot plot from Stella-EpiSCs, compared with non-transgenic controls. (**E**) Immunofluorescence analysis of Stella expression in a representative colony of Stella-EpiSCs; nuclei were stained with DAPI (blue). Insets show Stella$^+$ cells at a higher magnification. (**F**) Single cell Q-PCR analysis of PGC-marker gene expression in FACS-sorted Blimp1$^-$, Blimp1$^+$ and Stella$^+$ cells. Blimp1$^-$ and Blimp1$^+$ cells shown were further selected for the expression of Oct4. *y*-axis shows Ct (Cycle threshold) value for expression by Q-PCR. (**G**) Co-expression of Blimp1 and Oct4 in Stella$^+$ EpiSCs. Stella$^+$ cells (arrows) express both Blimp1-GFP and Oct4. Some Blimp1-GFP$^+$/Oct4$^+$ cells are negative for Stella (arrowheads). Scale bars: 20 μm.

2006). We detected Stella-GFP expression in a small proportion (0-1.5%) of cells in cultures of Stella-EpiSCs (Fig. 1D); these cells were also positive for the endogenous Stella protein (Fig. 1E). We first observed Stella-GFP$^+$ cells as early as the third passage of Stella-EpiSC cultures. Such Stella-GFP$^+$ cells were consistently observed for at least 42 passages in all the Stella-EpiSC lines. The proportion of cells that were detected as Stella-GFP$^+$ consistently ranged between 0-1.5% by FACS analysis regardless of the passage number Stella-EpiSCs. Q-PCR analysis using single cells confirmed that Stella-GFP$^+$ cells were positive for other markers of early germ cells, including *Blimp1*, *Dnd1*, *Nanos3* and *Prdm14*, the latter in particular is another key regulator of PGC specification (Fig. 1F) (Yamaji et al., 2008). These cells, as expected, were confined within the Blimp1$^+$ population, as confirmed by immunostaining in which all the Stella$^+$ cells (120/120) were also positive for Blimp1-GFP and Oct4 (Fig. 1G; data not shown). These results demonstrate that we could detect germ cells at distinct stages of development: from the initial Blimp1$^+$ PGC-precursors to the Stella-GFP$^+$ cells detected at the completion of specification process.

Next, we investigated the origin of the PGC population in more detail, beginning with the appearance of Blimp1-GFP$^+$ cells in EpiSC cultures. We therefore started with Blimp1-GFP$^-$ cells isolated by FACS-sorting, and monitored the appearance of Blimp1-GFP$^+$ PGC precursor cells. Indeed, although there were only a few Blimp1-GFP$^+$ cells after day 1 of culture, we found a progressive increase in the appearance of Blimp1$^+$/Oct4$^+$ cells on days 3 and 5 of culture (Fig. 2A,B). As expected, the Stella-expressing cells were detected at a later time, at least 5 days after the start of culture (Fig. 2A,B). These results demonstrate that Stella$^+$ cells in EpiSC culture were derived from the Blimp1-GFP$^-$ population via the Blimp1-GFP$^+$/Oct4$^+$ PGC precursor population; this sequence of events resembles PGC specification in vivo (Hayashi et al., 2007; Kurimoto et al., 2008; Ohinata et al., 2005).

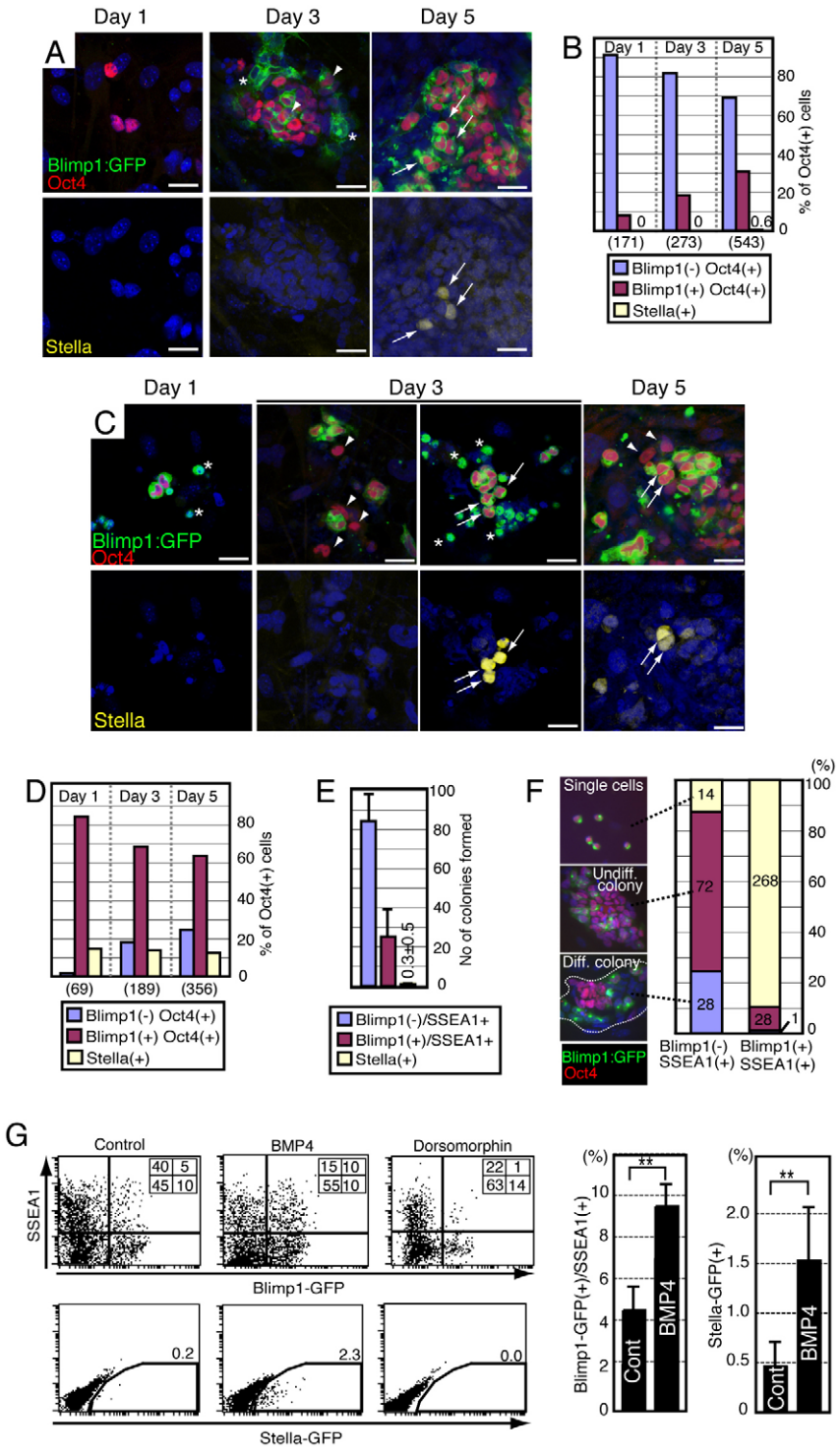

Fig. 2. Derivation of PGCs from EpiSCs. (**A**) Blmp1-GFP$^+$ cells originate from Blimp1-GFP$^-$ cells: FACS-sorted Blimp1-GFP$^-$ EpiSCs (estimated as 99% pure) were cultured for 1, 3 and 5 days, and stained with antibodies as indicated, and DAPI for nuclei (blue). Arrowheads and asterisks indicate representative Blimp1-GFP$^+$/Oct4$^+$ and Blimp1-GFP$^+$/Oct4$^-$ cells, respectively. Arrows indicate representative Stella$^+$ cells. Scale bar: 20 μm. (**B**) Bar graph showing the percentage of different cell types observed following culture of EpiSCs described in Fig. 1A. The total numbers of cells counted are shown below the graph. The passage number of Blimp1-EpiSCs used ranged between 14 and 22. (**C**) Blimp1-GFP$^+$/SSEA1$^+$ cells revert to Blmp1-GFP$^-$ cells: FACS-sorted Blimp1-GFP$^+$ EpiSCs (estimated purity was 97%) were cultured for 1, 3 and 5 days, and stained using antibodies as indicated, and DAPI for nuclei (blue). Note that Blimp1-GFP$^-$/Oct4$^+$ cells (arrowheads) appear de novo. Arrows indicate representative Stella$^+$ cells; asterisks indicate Blimp1-GFP$^+$ cells that are presumably undergoing cell death. Scale bar: 20 μm. (**D**) Detection of cells (%) in each population resulting from the culture of FACS-sorted Blimp1-GFP$^+$ EpiSCs. The numbers below the graph represent total number of cells counted. The passage number of Blimp1-EpiSCs used in this analysis ranged between 14 and 22. (**E**) The efficiency of colony formation for each cell population for 2000 FACS-sorted cells. Mean values were calculated from three independent experiments. (**F**) Types of cells/colonies detected after 3 days of culture. On the left are representative images of different types of cells/colonies stained using antibodies as indicated, and DAPI for nuclei (blue). The bar graph on the right shows the percentage of each type of cell/colony after 3 days of culture using FACS-sorted cells as indicated. (**G**) Effect of BMP-mediated pathway on PGCs detected in EpiSC cultures. Shown are FACS analyses depicting the proportion of Blimp1-GFP$^+$ and SSEA1$^+$ cells (upper row), and Stella-GFP$^+$ cells (lower row) in response to BMP4 and dorsomorphin (1 μM) treatment. The bar graph on the right summarises the results of FACS analyses. The differences are statistically significant (P<0.01, Student's t-test); mean values were calculated from at least three independent experiments.

Our observations so far indicate that EpiSCs maintained under culture conditions that promote their self-renewal without compromising their pluripotency (as judged by the expression of Oct4) can continually generate a population of PGCs, which raised the question of how the balance between different subpopulations is maintained. According to some recently suggested models, it appears that stem cells can fluctuate between different epigenetic and phenotypical states while undergoing self-renewal in culture (Enver et al., 2009; Graf and Stadtfeld, 2008; Hayashi et al., 2008). To address this issue concerning the emergence of PGCs from EpiSCs, we examined the fate of FACS-sorted Blimp1-GFP$^+$/SSEA1$^+$ and Stella-GFP$^+$ cells. We found that the culture of isolated Blimp1-GFP$^-$/Oct4$^+$ cells gradually showed an increase in the number of colonies at days 3-5 of culture (Fig. 2C,D). By contrast, the Blimp1-GFP$^+$/SSEA1$^+$ cells showed poor colony formation (Fig. 2E); indeed many of these cells remained as single cells (Fig. 2F). This result demonstrates the existence of a dynamic equilibrium in EpiSCs, in which some Blimp1-GFP$^+$/SSEA1$^+$ cells maintain the potential to revert to Blimp1-GFP$^-$/Oct4$^+$ cells. Considering our observation that differentiation of PGCs from

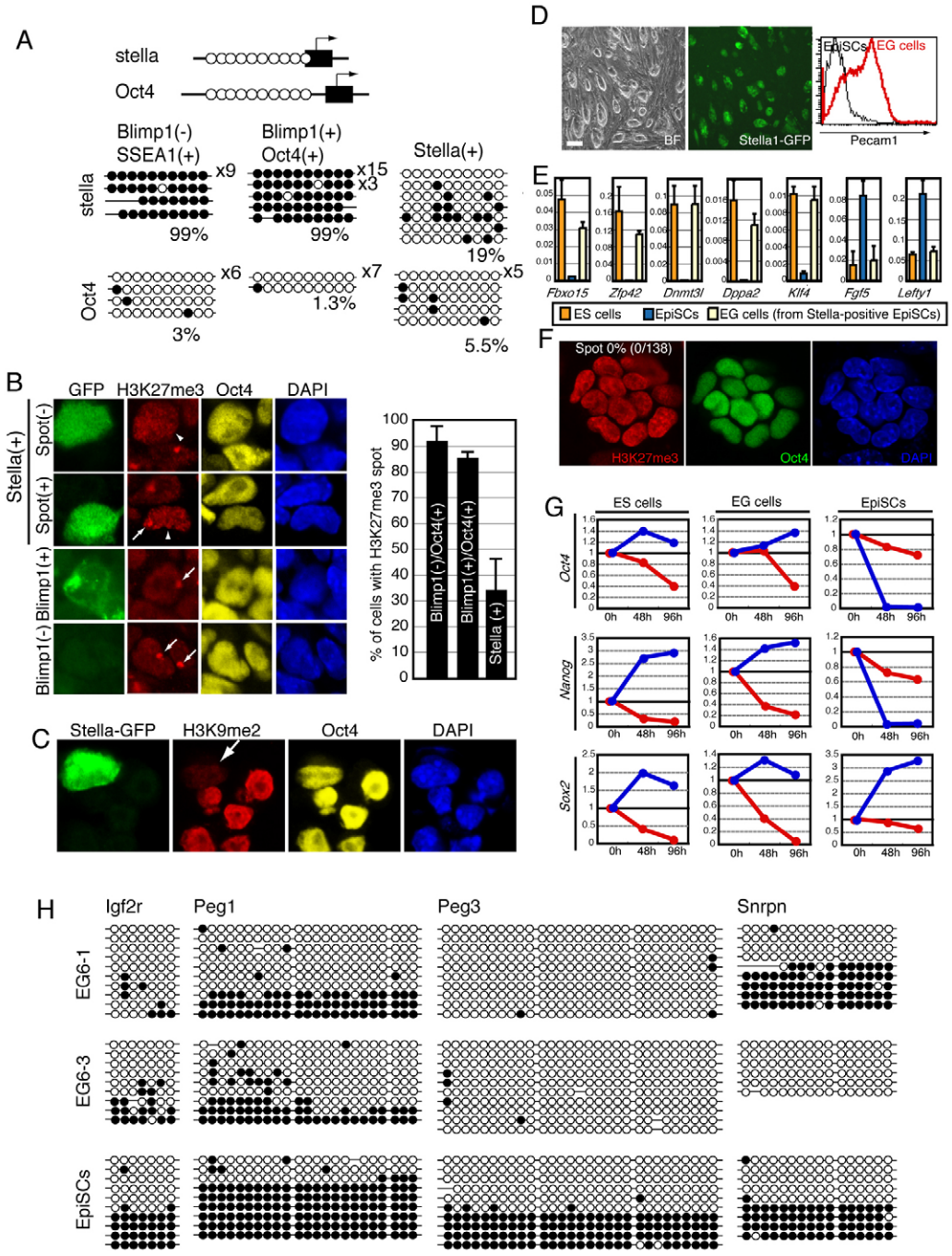

Fig. 3. Epigenetic reprogramming during PGC specification from EpiSCs. (**A**) Bisulphite sequencing analysis of *Stella* and *Oct4* loci in different populations. CpG sequences shown at the top became methylated (black circles) or unmethylated (white circles); the extent of methylation (%) is indicated below the profiles. (**B**) Loss of H3K27me3 'spot' (depicted by arrows) in Stella-GFP$^+$ cells. Stella-GFP$^+$ cells (arrowheads) possess elevated levels of H3K27me3. The bar graph on the right is a summary of the percentage of cells with detectable H3K27me3 spot in each cell population. (**C**) Downregulation of H3K9me2 (red) in Stella-GFP$^+$ cells; arrow indicates a representative Stella-GFP$^+$ cell that has low levels of H3K9me2. (**D**) Derivation of EGC cells from Stella$^+$ cells from EpiSCs. Shown are images of EGCs in bright field (left), GFP expression (middle) and FACS analysis for Pecam1 expression (right). Scale bar: 100 μm. (**E**) Gene expression analysis of ESCs, EpiSCs and EGCs (derived from Stella-GFP$^+$EpiSCs). Included is the analysis of genes that are differentially expressed in ESCs and EpiSCs (Brons et al., 2007; Hayashi et al., 2008; Tesar et al., 2007). Note similarities in gene expression between ESCs and EGCs. (**F**) Immunofluorescence staining for H3K27me3. Shown is a colony of Stella$^+$ female EGCs generated from in vitro-derived PGCs emerging from EpiSCs. The cells were stained with H3K27me3 antibody (red), Oct4 (green) and DAPI (blue). Amongst 138 Oct4$^+$ EGCs counted, all cells lack a H3K27me3 'spot'. (**G**) Characterisation of key signalling pathways for the maintenance of pluripotent gene expression. ESCs, EGCs (derived from Stella-GFP$^+$EpiSC) and EpiSCs were cultured with either JAK inhibitor I (1 μM)/dorsomorphin (1 μM; red lines) or SB431542 (10 μM)/PD184531 (0.5 μM)/SU5402 (1 μM; blue lines). Graphs show relative levels of expression at 0 hours, 48 hours and 96 hours after the addition of inhibitors. Expression was normalised to the levels detected at 0 hours in each case. (**H**) Bisulphite sequencing analyses of imprinted gene loci in two independent EGC clones (derived from Stella-GFP$^+$EpiSCs) and EpiSCs. The locations of CpG sequences in each gene were described previously (Lucifero et al., 2002). CpG sequences are shown by black (methylated) and white (unmethylated) circles.

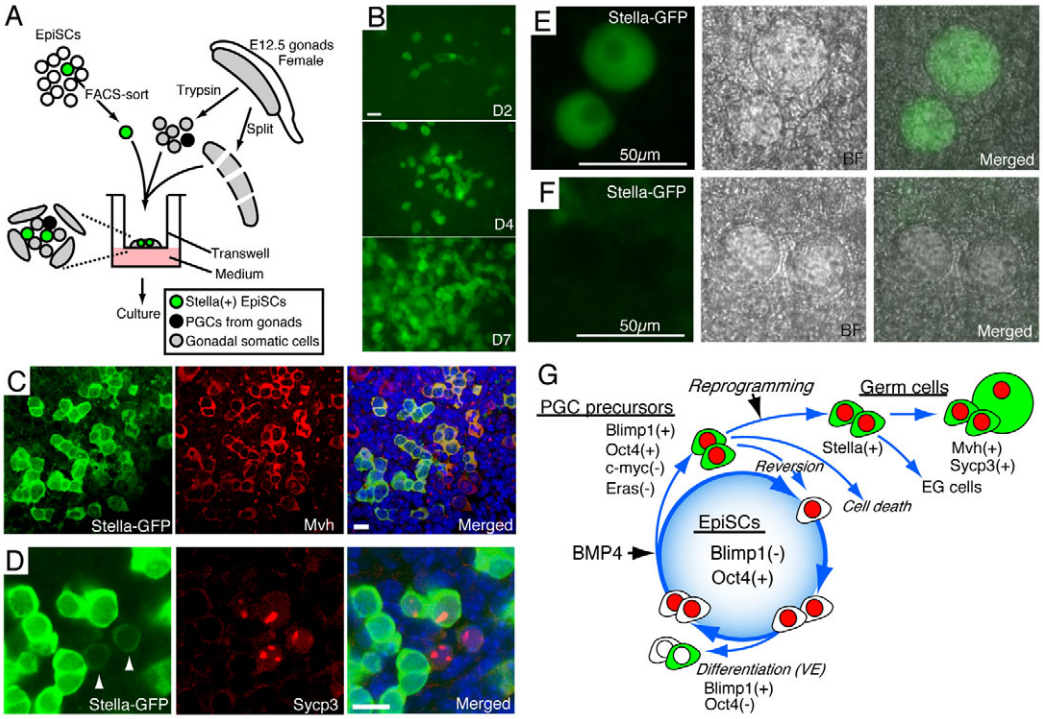

Fig. 4. Differentiation of PGCs from Stella-EpiSCs. (**A**) Experimental design for the culture of FACS-sorted Stella-GFP$^+$ PGCs, with dissociated cells from E12.5 female gonads containing both somatic and germ cells, together with pieces of the gonadal tissues. (**B**) Proliferation of Stella-GFP$^+$ cells, shown in representative images at day 2 (D2), day 4 (D4) and day 7 (D7) of culture. Scale bar: 20 μm. (**C**,**D**) Differentiation of Stella-GFP$^+$ cells. Shown are immunofluorescence images for Stella, DAPI (blue), Mvh (C) or Sycp3 (D). Arrowheads in D indicate Sycp3$^+$ cells that exhibit a reduction in Stella-GFP expression. Scale bar: 20 μm. (**E**,**F**) Development of oocyte-like structures in culture with gonadal cells. Representative images of growing primary oocytes following culture of Stella-GFP$^+$ (E), compared with those from control endogenous (F) PGCs. (**G**) Model illustrating delineation of PGCs from self-renewing pluripotent EpiSCs. Blimp1$^+$/Oct4$^+$ PGC precursors emerge continuously from EpiSCs, which revert to Blimp1$^-$ cells, undergo cell death, or commit to Stella$^+$ PGCs. Following epigenetic reprogramming, these cells develop as Stella$^+$ PGCs, which in turn could be induced to undergo dedifferentiation into EGCs, which resemble ESCs and not EpiSCs (see text for details).

EpiSCs is accomplished in a stepwise manner (Fig. 1F), it is likely that the reversible population of Blimp1-GFP$^+$/SSEA1$^+$ cells is at an early stage of their progression towards PGCs, and lack expression of later markers of germ cells, such as *Prdm14* and *Dnd1*. At day 3 and day 5 of culture of Blimp1-GFP$^+$/SSEA1$^+$ cells, ~20% showed strong expression of Stella (Fig. 2C,D), while others with dense nuclei were presumably dying. Counts of living single cells and colonies at day 3 of culture showed that approximately 90% (268/297) of the sorted Blimp1-GFP$^+$/SSEA1$^+$ cells stayed as single cells, while around 10% (29/297) of the cells formed colonies and reverted to Blimp1$^-$/Oct4$^+$ cells. By contrast, around 90% (100/114) of Blimp1-GFP$^-$/SSEA1$^+$ cells formed colonies (Fig. 2F). Furthermore, differentiated colonies containing Blimp1$^+$/Oct4$^-$ cells, which represent the VE cells, were more frequently seen in cultures of Blimp1-GFP$^-$/SSEA1$^+$ cells (Fig. 2F). Notably, unlike Blimp1$^+$/SSEA1$^+$ cells, Stella-GFP$^+$ cells could not form colonies, and eventually died under EpiSC culture conditions (Fig. 2E).

Based on the combined observations, it appears that EpiSCs are in a state of dynamic equilibrium in which the delineation of PGC precursors and specified PGCs occurs continually. In EpiSCs, the Blimp1-GFP$^-$ cells represent the pluripotent cells, which, in part, differentiate into Blimp1$^+$ PGC precursors, followed by the formation of Stella$^+$ PGCs. By contrast, Blimp1-GFP$^+$/SSEA1$^+$ PGC precursors are predominantly poised towards the germ cell fate, and some of these cells go through to complete the specification process, whereas others undergo apoptosis or revert back to Blimp1$^-$/Oct4$^+$ cells. Consistent with this interpretation, we found that *Myc* (also known as *c-myc*) and *Eras* were dramatically downregulated in the Blimp1$^+$/Oct4$^+$ cells (see Fig. S3 in the supplementary material). *Myc* is a putative target of Blimp1 and its downregulation is thought to result in a slowing down of the cell cycle of PGCs (Lin et al., 1997; McLaren and Lawson, 2005). *Eras* is a known regulator of ESC proliferation (Takahashi et al., 2003). Thus, downregulation of these genes might result in poor proliferation and colony formation of Blimp1$^+$/Oct4$^+$ cells.

Because Bmp4 is a key signal for PGC specification (Lawson et al., 1999), we sought to determine whether this signalling molecule could influence PGC formation from EpiSCs. It should be noted that although we had not added any recombinant BMP4 to our culture medium, EpiSCs themselves express Bmp4. We therefore added Dorsomorphin, an inhibitor of BMP signalling (Yu et al., 2008) to EpiSC cultures to monitor the effect on PGC derivation. Indeed, addition of Dorsomorphin to EpiSCs in culture reduced the proportion of both the Stella$^+$ and the Blimp1$^+$/SSEA1$^+$ cells (Fig. 2G). Conversely, addition of recombinant BMP4 induced a small but significant increase in the proportion of Stella-GFP$^+$ cells, as well as of the Blimp1$^+$/SSEA1$^+$ cells (Fig. 2G). However, we did not detect significant PGC induction when BMP8b was added simultaneously with BMP4 in the culture (data not shown). These results demonstrate that BMP4 is at least one of the key cytokines present in the culture,

and may promote PGC formation from EpiSCs. It is possible that localised activation of BMP-Smad signalling in EpiSCs produces an appropriate microenvironment in which PGC precursors might be delineated in response to the signalling. This is likely as in human ES cells (hESCs), which resemble EpiSCs, the levels of phosphorylated Smad1 are variable in individual colonies, and this causes their heterogeneous response to differentiation (Peerani et al., 2007).

We next investigated whether appropriate epigenetic reprogramming events occur in the PGC derived from EpiSCs. First, we determined the DNA methylation status of the pluripotent genes *Stella*, *Rex1* (also known as *Zfp42*) and *Fbxo15*, all of which are hypermethylated in EpiSCs (Fig. 3A; see also Fig. S4 in the supplementary material), but not in ESCs (Hayashi et al., 2008; Imamura et al., 2006). Strikingly, the *Stella* locus becomes hypomethylated during the transition from Blmp1$^+$/Oct4$^+$ to Stella$^+$ cells (Fig. 3A); this was also the case with *Rex1* and *Fbxo15* loci (see Fig. S4 in the supplementary material), demonstrating that PGC specification from EpiSCs is coupled with DNA demethylation of these loci. This epigenetic change is an indicator of an important reprogramming event (Seki et al., 2005), which helps to erase the epigenetic memory of EpiSCs. Concomitantly, the de novo DNA methyltransferase Dnmt3b was downregulated in Stella$^+$ EpiSCs (see Fig. S3 in the supplementary material), which is consistent with similar observations on nascent PGCs in vivo (Yabuta et al., 2006). Although the precise effect of loss of Dnmt3b on reprogramming remains to be elucidated, this may be an essential step towards later epigenetic changes in germ cells.

Considering that the onset of Stella expression in PGCs in EpiSC cultures is associated with an irreversible cell fate decision towards PGCs, we expected other key epigenetic changes in these cells, including reactivation of the inactive X chromosome in emerging EpiSCs. Indeed, most of the Blimp1$^-$/Oct4$^+$ and Blimp1$^+$/Oct4$^+$ cells exhibited accumulation of tri-methyl histone H3 lysine 27 (H3K27me3), which is diagnostic for the inactive X chromosome (Fig. 3B, arrows). By contrast, H3K27me3 spot was detectable in only about 30% of Stella$^+$ cells, indicating the commencement of X-reactivation. In addition, global levels of H3K27me3 increased (Fig. 3B, arrowhead), but the levels of histone H3 lysine 9 (H3K9me2) decreased in the Stella$^+$ cells (Fig. 3C), as is the case in nascent PGCs in vivo (Hajkova et al., 2008; Seki et al., 2005). Consistently, the levels of *Glp* transcripts were downregulated [*Glp* encodes a protein that together with G9a is essential for H3K9me2 methylation (Tachibana et al., 2005); also known as *Ehmt1* – Mouse Genome Informatics; see Fig. S3 in the supplementary material]. These changes are amongst the first steps towards extensive epigenetic reprogramming events in germ cells.

Pluripotent EGCs, which exhibit striking similarities to ESCs, can be derived from PGCs (Matsui et al., 1992; Resnick et al., 1992). Notably, PGCs acquire the potential to dedifferentiate into EGCs after E8.5, when the appropriate epigenetic reprogramming process is completed (Hayashi and Surani, 2009). To evaluate whether PGCs from EpiSCs can undergo such reprogramming, we cultured FACS-sorted Stella-GFP$^+$ cells under conditions that promote the derivation of EGCs (see Materials and methods). We performed four independent culture experiments using 3000 Stella-GFP$^+$ cells in each experiment, which resulted in the derivation of three EGC lines from independent Stella-EpiSC clones. Compared with EGC derivation from PGCs isolated from embryos in vivo (Matsui et al., 1992; Resnick et al., 1992), the derivation frequency from Stella$^+$ cells in vitro was less efficient (data not shown). Nevertheless, these EGCs derived from EpiSCs showed appropriate gene expression and epigenetic changes. For example, we detected re-expression of Stella and Pecam1, which are not expressed in EpiSCs (Fig. 3D). Q-PCR analysis of other marker genes further confirmed that the EGCs from Stella-GFP$^+$ cells were similar to ESCs and clearly distinguishable from EpiSCs (Fig. 3E). Furthermore, we could no longer detect accumulation of H3K27me3 in these EGCs (Fig. 3F). The signalling pathway involved in the self-renewal of EGCs switched to LIF/Bmp4 (as is the case for ESC) from the bFGF/Activin that is required for EpiSCs (Fig. 3G). Thus, cumulative evidence demonstrates that intrinsic reprogramming events during the formation of PGCs in vitro converts the epigenetic state of EpiSCs to that of EGCs, which is equivalent to ESCs. We exclude the possibility, however unlikely, that EpiSCs could directly dedifferentiate into ESC-like cells under these culture conditions, as bisulphite sequence analysis of EGCs revealed the erasure of allelic DNA methylation associated with the imprinted gene loci, supporting the case for their origin from PGCs (Fig. 3H).

Finally, we went on to investigate whether the Stella$^+$ cells can be induced to proliferate and undergo further development in vitro, which is restricted under EpiSC culture conditions. To investigate this possibility, we co-cultured Stella-GFP$^+$ cells with E12.5 female gonadal cells, which also contained endogenous germ cells. This showed that the in vitro generated PGCs were able to proliferate and develop further (Fig. 4A,B). We found that clumps of Stella-GFP$^+$ cells, which probably originated from single cells, were composed of between two and ten cells after 7 days of culture (Fig. 4B,C), indicating that they had undergone up to four cell divisions. After 7-10 days of culture, we detected expression of the mouse vasa homologue Mvh (Ddx4 – Mouse Genome Informatics; Fig. 4C), as well as of Sycp3, a marker of meiosis, in the Stella-GFP$^+$ cells (Fig. 4D). We also observed a progressive reduction in the levels of Stella-GFP expression in some of the Sycp3$^+$ cells (Fig. 4D), suggesting that these cells had undergone further differentiation, similar to the events decribed in vivo (Sato et al., 2002). After about 40 days in culture, we observed oocyte-like cells with strong expression of Stella-GFP and a characteristically large nucleus (Fig. 4E). However, the efficiency of the formation oocyte-like cells was very low (0.6±0.8 oocyte-like cells/3000 Stella-GFP$^+$ cells; n=6), although these cells were morphologically indistinguishable from oocytes that developed from the endogenous germ cells present in the same co-cultures (Fig. 4F). These results demonstrate that Stella$^+$ cells originating from EpiSCs have the key hallmarks of the germ cell lineage.

Our study shows that self-renewing EpiSCs, unlike ESCs, produce a continuous stream of PGCs in vitro (Fig. 4G) that can potentially generate an infinite number of germ cells. The emergence of PGCs from EpiSCs in vitro is accompanied by appropriate epigenetic reprogramming events. Notably, the intrinsic reprogramming associated with PGC specification results in the erasure of the epigenetic memory of EpiSCs. This is evident because EGCs derived from PGCs resemble ESCs and not EpiSCs, suggesting that they acquire an earlier ICM-like epigenetic state. This in vitro model for the derivation of PGCs from EpiSCs will be particularly useful for investigations on the underlying mechanisms of epigenetic reprogramming events in early germ cells. The fact that EpiSCs resemble hESCs also raises a possibility that our investigation could be extended to hESCs, with the prospect of studying the earliest stages of the human germ cell lineage.

Acknowledgements

We thank Drs Mitinori Saitou and Shinichiro Chuma for Blimp1-GFP mice and the Sycp3 antibody, respectively. This work was supported by the Japan Society for Promotion of Science to K.H. and the Wellcome Trust (062801). Deposited in PMC for release after 6 months.

Supplementary material

Supplementary material for this article is available at http://dev.biologists.org/cgi/content/full/136/21/3549/DC1

References

Ancelin, K., Lange, U. C., Hajkova, P., Schneider, R., Bannister, A. J., Kouzarides, T. and Surani, M. A. (2006). Blimp1 associates with Prmt5 and directs histone arginine methylation in mouse germ cells. *Nat. Cell Biol.* **8**, 623-630.

Brons, I. G., Smithers, L. E., Trotter, M. W., Rugg-Gunn, P., Sun, B., Chuva de Sousa Lopes, S. M., Howlett, S. K., Clarkson, A., Ahrlund-Richter, L., Pedersen, R. A. et al. (2007). Derivation of pluripotent epiblast stem cells from mammalian embryos. *Nature* **448**, 191-195.

Chuva de Sousa Lopes, S. M., Hayashi, K., Shovlin, T. C., Mifsud, W., Surani, M. A. and McLaren, A. (2008). X chromosome activity in mouse XX primordial germ cells. *PLoS Genet.* **4**, e30.

de Napoles, M., Nesterova, T. and Brockdorff, N. (2007). Early loss of Xist RNA expression and inactive X chromosome associated chromatin modification in developing primordial germ cells. *PLoS ONE* **2**, e860.

Durcova-Hills, G. and Surani, A. (2008). Reprogramming primordial germ cells (PGC) to embryonic germ (EG) cells. *Curr. Protoc. Stem Cell Biol.* **Chapter 1**, Unit1A.3.

Durcova-Hills, G., Tang, F., Doody, G., Tooze, R. and Surani, M. A. (2008). Reprogramming primordial germ cells into pluripotent stem cells. *PLoS ONE* **3**, e3531.

Enver, T., Pera, M., Peterson, C. and Andrews, P. W. (2009). Stem cell states, fates, and the rules of attraction. *Cell Stem Cell* **4**, 387-397.

Evans, M. J. and Kaufman, M. H. (1981). Establishment in culture of pluripotential cells from mouse embryos. *Nature* **292**, 154-156.

Graf, T. and Stadtfeld, M. (2008). Heterogeneity of embryonic and adult stem cells. *Cell Stem Cell* **3**, 480-483.

Guo, G., Yang, J., Nichols, J., Hall, J. S., Eyres, I., Mansfield, W. and Smith, A. (2009). Klf4 reverts developmentally programmed restriction of ground state pluripotency. *Development* **136**, 1063-1069.

Hajkova, P., Ancelin, K., Waldmann, T., Lacoste, N., Lange, U. C., Cesari, F., Lee, C., Almouzni, G., Schneider, R. and Surani, M. A. (2008). Chromatin dynamics during epigenetic reprogramming in the mouse germ line. *Nature* **452**, 877-881.

Hayashi, K. and Surani, M. A. (2009). Resetting the epigenome beyond pluripotency in the germ line. *Cell Stem Cell* **4**, 493-498.

Hayashi, K., de Sousa Lopes, S. M. and Surani, M. A. (2007). Germ cell specification in mice. *Science* **316**, 394-396.

Hayashi, K., de Sousa Lopes, S. M., Tang, F. and Surani, A. (2008). Dynamic equilibrium and heterogeneity of mouse pluripotent stem cells with distinct functional and epigenetic states. *Cell Stem Cell* **3**, 391-401.

Imamura, M., Miura, K., Iwabuchi, K., Ichisaka, T., Nakagawa, M., Lee, J., Kanatsu-Shinohara, M., Shinohara, T. and Yamanaka, S. (2006). Transcriptional repression and DNA hypermethylation of a small set of ES cell marker genes in male germline stem cells. *BMC Dev. Biol.* **6**, 34.

Kurimoto, K., Yabuta, Y., Ohinata, Y. and Saitou, M. (2007). Global single-cell cDNA amplification to provide a template for representative high-density oligonucleotide microarray analysis. *Nat. Protoc.* **2**, 739-752.

Kurimoto, K., Yabuta, Y., Ohinata, Y., Shigeta, M., Yamanaka, K. and Saitou, M. (2008). Complex genome-wide transcription dynamics orchestrated by Blimp1 for the specification of the germ cell lineage in mice. *Genes Dev.* **22**, 1617-1635.

Lawson, K. A., Dunn, N. R., Roelen, B. A., Zeinstra, L. M., Davis, A. M., Wright, C. V., Korving, J. P. and Hogan, B. L. (1999). Bmp4 is required for the generation of primordial germ cells in the mouse embryo. *Genes Dev.* **13**, 424-436.

Lin, Y., Wong, K. and Calame, K. (1997). Repression of c-myc transcription by Blimp-1, an inducer of terminal B cell differentiation. *Science* **276**, 596-599.

Lucifero, D., Mertineit, C., Clarke, H. J., Bestor, T. H. and Trasler, J. M. (2002). Methylation dynamics of imprinted genes in mouse germ cells. *Genomics* **79**, 530-538.

Matsui, Y., Zsebo, K. and Hogan, B. L. (1992). Derivation of pluripotential embryonic stem cells from murine primordial germ cells in culture. *Cell* **70**, 841-847.

McLaren, A. and Lawson, K. A. (2005). How is the mouse germ-cell lineage established? *Differentiation* **73**, 435-437.

Niwa, H. (2007). How is pluripotency determined and maintained? *Development* **134**, 635-646.

Ohinata, Y., Payer, B., O'Carroll, D., Ancelin, K., Ono, Y., Sano, M., Barton, S. C., Obukhanych, T., Nussenzweig, M., Tarakhovsky, A. et al. (2005). Blimp1 is a critical determinant of the germ cell lineage in mice. *Nature* **436**, 207-213.

Payer, B., Chuva de Sousa Lopes, S. M., Barton, S. C., Lee, C., Saitou, M. and Surani, M. A. (2006). Generation of stella-GFP transgenic mice: A novel tool to study germ cell development. *Genesis* **44**, 75-83.

Peerani, R., Rao, B. M., Bauwens, C., Yin, T., Wood, G. A., Nagy, A., Kumacheva, E. and Zandstra, P. W. (2007). Niche-mediated control of human embryonic stem cell self-renewal and differentiation. *EMBO J.* **26**, 4744-4755.

Resnick, J. L., Bixler, L. S., Cheng, L. and Donovan, P. J. (1992). Long-term proliferation of mouse primordial germ cells in culture. *Nature* **359**, 550-551.

Saitou, M., Barton, S. C. and Surani, M. A. (2002). A molecular programme for the specification of germ cell fate in mice. *Nature* **418**, 293-300.

Sato, M., Kimura, T., Kurokawa, K., Fujita, Y., Abe, K., Masuhara, M., Yasunaga, T., Ryo, A., Yamamoto, M. and Nakano, T. (2002). Identification of PGC7, a new gene expressed specifically in preimplantation embryos and germ cells. *Mech. Dev.* **113**, 91-94.

Seki, Y., Hayashi, K., Itoh, K., Mizugaki, M., Saitou, M. and Matsui, Y. (2005). Extensive and orderly reprogramming of genome-wide chromatin modifications associated with specification and early development of germ cells in mice. *Dev. Biol.* **278**, 440-458.

Seki, Y., Yamaji, M., Yabuta, Y., Sano, M., Shigeta, M., Matsui, Y., Saga, Y., Tachibana, M., Shinkai, Y. and Saitou, M. (2007). Cellular dynamics associated with the genome-wide epigenetic reprogramming in migrating primordial germ cells in mice. *Development* **134**, 2627-2638.

Sugimoto, M. and Abe, K. (2007). X chromosome reactivation initiates in nascent primordial germ cells in mice. *PLoS Genet.* **3**, e116.

Surani, M. A., Hayashi, K. and Hajkova, P. (2007). Genetic and epigenetic regulators of pluripotency. *Cell* **128**, 747-762.

Tachibana, M., Ueda, J., Fukuda, M., Takeda, N., Ohta, T., Iwanari, H., Sakihama, T., Kodama, T., Hamakubo, T. and Shinkai, Y. (2005). Histone methyltransferases G9a and GLP form heteromeric complexes and are both crucial for methylation of euchromatin at H3-K9. *Genes Dev.* **19**, 815-826.

Takahashi, K., Mitsui, K. and Yamanaka, S. (2003). Role of ERas in promoting tumour-like properties in mouse embryonic stem cells. *Nature* **423**, 541-545.

Tesar, P. J., Chenoweth, J. G., Brook, F. A., Davies, T. J., Evans, E. P., Mack, D. L., Gardner, R. L. and McKay, R. D. (2007). New cell lines from mouse epiblast share defining features with human embryonic stem cells. *Nature* **448**, 196-199.

Yabuta, Y., Kurimoto, K., Ohinata, Y., Seki, Y. and Saitou, M. (2006). Gene expression dynamics during germline specification in mice identified by quantitative single-cell gene expression profiling. *Biol. Reprod.* **75**, 705-716.

Yamaji, M., Seki, Y., Kurimoto, K., Yabuta, Y., Yuasa, M., Shigeta, M., Yamanaka, K., Ohinata, Y. and Saitou, M. (2008). Critical function of Prdm14 for the establishment of the germ cell lineage in mice. *Nat. Genet.* **40**, 1016-1022.

Yu, P. B., Hong, C. C., Sachidanandan, C., Babitt, J. L., Deng, D. Y., Hoyng, S. A., Lin, H. Y., Bloch, K. D. and Peterson, R. T. (2008). Dorsomorphin inhibits BMP signals required for embryogenesis and iron metabolism. *Nat. Chem. Biol.* **4**, 33-41.